

StyLandGAN: A StyleGAN based Landscape Image Synthesis using Depth-map

Gunhee Lee Jonghwa Yim Chanran Kim Minjae Kim
 Vision AI Lab, AI Center, NCSOFT
 {victorleee, jonghwayim, chanrankim, minjaekim}@ncsoft.com



Figure 1. Our proposed StyLandGAN framework can synthesize diverse structure and style landscape images from a single segmentation map. **(Left)** Our ‘2-phase inference’ firstly generates diverse depth maps from a single segmentation map (Phase1:S2D), and then generates landscape images from both segmentation and depth map inputs (Phase2:SD2I). **(Right)** We also show that shifting the local region of the depth map (Here, the sky and mountain areas) can achieve the desired result.

Abstract

Despite recent success in conditional image synthesis, prevalent input conditions such as semantics and edges are not clear enough to express ‘Linear (Ridges)’ and ‘Planar (Scale)’ representations. To address this problem, we propose a novel framework StyLandGAN, which synthesizes desired landscape images using a depth map which has higher expressive power. Our StyleLandGAN is extended from the unconditional generation model to accept input conditions. We also propose a ‘2-phase inference’ pipeline which generates diverse depth maps and shifts local parts so that it can easily reflect user’s intend. As a comparison, we modified the existing semantic image synthesis models to accept a depth map as well. Experimental results show that our method is superior to existing methods in quality, diversity, and depth-accuracy.

1. Introduction

Visual contents creation tools have been developed to allow users to embody their own abstract ideas into concrete

images. In particular, tools for landscape creation are also spotlighted in the field of environment concept art, which shows a glimpse of world in computer games [22]. These tools are developed mainly in the name of ‘conditional image synthesis’ based on GANs [6].

Although previous conditional models can synthesize visually pleasing landscape images either from segmentation map or edge scribbles (Sec. 2), these conditional inputs are not sufficient to convey user’s intention due to low expressive power. Comparison between conditional inputs is shown in Figure 2. Although most of the previous works use **segmentation map** to control the contents of the image, it does not contain both linear (Ridge) and planar (Scale, Texture) representations. There are also works exploiting **edge scribbles** to control images. Even if humans can perceive depth from edge drawings [7], the edge itself lacks planar representation which leads to depth ambiguity. Therefore, synthesizing landscape images only from those inputs leaves depth representation unclear. Unlike these input modalities, we observe that **depth map** can express both linear and planar representations. Furthermore, with recent improvements in monocular depth map estimation [4,5,20,25], it becomes much easier to acquire a pseudo

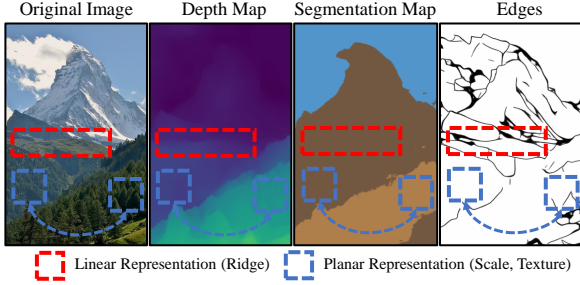


Figure 2. Comparison between various input modalities. A depth map can express both ridge (red) and scale (blue) information. Segmentation is hard to handle ridge, and edge is difficult to express scale information.

depth map even from a single image. Thus, one can build an image-depth pair dataset without any ground truth depth maps.

In this paper, we present the StyLandGAN framework that uses multiple input conditions including segmentation and depth map to convey user intentions. Our framework extends the previous StyleMapGAN [13] as a conditional-GAN framework. In order to synthesize landscape images, we first suggest a segmentation and depth-to-image translation model (SD2I). Moreover, we propose a segmentation-to-depth translation model (S2D) which provides diverse global depth suggestions for users to acquire the desired depth map more easily. In addition, we design a segment-wise depth shift technique to enable local region editing. Combining all of the above, we provide a ‘2-phase inference’ pipeline that first generates structure information using S2D translation, edits local parts if needed, and finally generates landscape images using SD2I translation. Experimental results show that StyLandGAN outperforms previous works with an identical depth map input setting.

2. Related Work

Image Synthesis Approach. Image synthesis has been developed using two different approaches. The first approach is the *create-from-simple* approach. This method generates a complex image from a relatively simple condition input. This scheme can have various input modalities, from semantic segmentation map [3, 11, 17, 22, 28], edges [1, 11], or even from text prompts [24, 26, 29]. There are also methods using various conditional inputs [3, 10, 21]. Secondly, with the *choose-from-many* approach, multiple images may be created from a single input. In the line of research on image-to-image translation (I2I), many approaches have been developed not only for single-modal translation [11, 14, 22, 31, 33, 37] but also for multi-modal translation [2, 9, 15, 16, 27, 36]. Our framework is designed to use both approaches, which starts with simple condition

input, then outputs relatively complex multiple outputs.

Representation Disentanglement. Previous I2I translation research has attempted to separate ‘content information’ and ‘style information’ in the image [2, 9, 15, 16, 23, 27]. However, this separation is an ill-defined and ill-posed problem. As suggested in [21], we also define the conditioning information as ‘content’. This approach leads to define ‘style’ as information that contents do not capture. To be more specific in our segmentation and depth-to-image translation (SD2I) model, it can be said that depth and segmentation maps are mainly responsible for content information and the rest are style information.

3. StyLandGAN

Our goal is to obtain a model capable of generating diverse images with a given conditions. Here, we describe our proposed model that exploits two different modalities, i.e., semantic segmentation and depth map. We propose StyLandGAN which adopts a *condition latent code*, an intermediate 2D spatial latent code representing segmentation and depth maps. We denote a single image as \mathcal{I} , and the corresponding segmentation map and depth map as \mathcal{S} , and \mathcal{D} , respectively.

3.1. StyLand Generator

Our generator consists of three components as shown in Figure 3: (1) Condition preparation module, (2) Condition fusion module, and (3) Image synthesis module. These three modules are composed separately, but sequentially the previous result is given to the next module to synthesize the final image.

Condition preparation module prepares random latent code and condition latent code separately. Thus, this module consists of mapping network for random latent code and condition blocks for condition latent codes. As in [13], our mapping network produces random latent code $w \in \mathbb{R}^{C_0 \times H_0 \times W_0}$ with initial spatial size. Each condition blocks firstly resizes input condition $\mathcal{S}, \mathcal{D} \in \mathbb{R}^{C \times H \times W}$ into $\mathcal{S}_i, \mathcal{D}_i \in \mathbb{R}^{C_i \times H_i \times W_i}$ for each i -th layer. Then, these resized maps are concatenated in channel-wise direction, and output condition latent code $m_i \in \mathbb{R}^{C_i \times H_i \times W_i}$ by convolution operation.

Condition fusion module merges random latent code w and condition latent code m_1 of the first layer by element-wise addition operation. Then, it outputs the intermediate latent code, w_1^+ by convolution operation for next layer. All the intermediate latent code $w_i^+ \in \mathbb{R}^{C_i \times H_i \times W_i}$ is passed to the i -th layer of image synthesis module, and also fused with the $(i + 1)$ -th condition latent code, m_{i+1} . This operation continues till it reaches the size of original image $\mathcal{I} \in \mathbb{R}^{C \times H \times W}$ to convey more detailed spatial information.

Finally, **Image synthesis module** progressively synthesizes image with affine transformed latent code of each

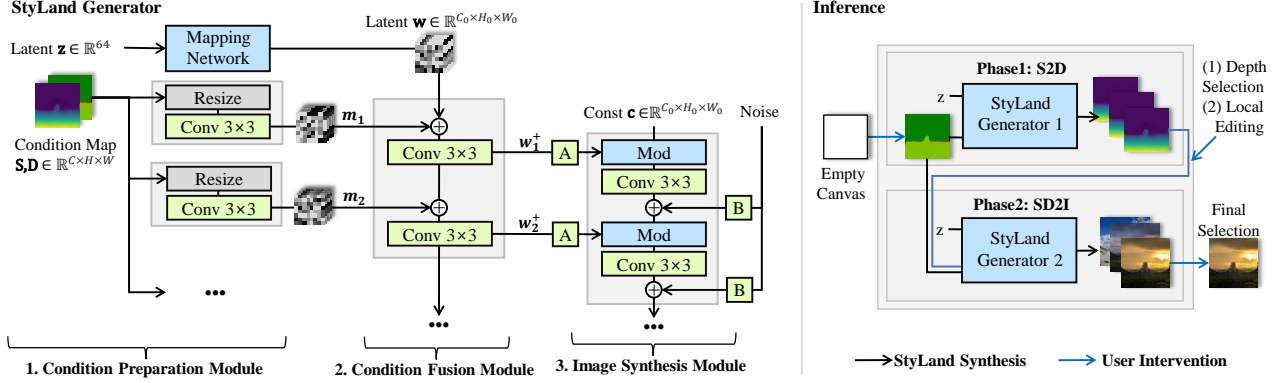


Figure 3. (Left) Our StyLand Generator composed of 3 different modules: condition preparation module, condition fusion module, and image synthesis module. (Right) Our ‘2-phase inference’ first generates depth of given segmentation map then generates final landscape output.

layer, w_i^+ . We add per-pixel noise which is introduced in [12], so that it can generate a diverse and delicate changes of landscape images.

We follow the training scheme procedure in StyleMapGAN [13] training scheme which uses adversarial loss [6], R1 regularization [19], Perceptual loss [34], Domain-guided loss [35], and reconstruction loss. Like [13], we also use the encoder and jointly train with generator and discriminator.

3.2. Depth Map Acquisition

As we have argued in Figure 2, a depth map is beneficial for handling linear and planar representation. However, it requires additional delicate effort to obtain the desired depth map. Thus, we suggest the global acquisition method ‘S2D translation’ and the local editing method ‘Segment-wise depth shift’ to acquire the desired depth map.

Global: S2D translation. We have argued a basic model that translates the segmentation map and depth map into the corresponding image, which is the SD2I translation model. Likewise, we also train the segmentation-to-depth (S2D) translation model, with an identical StyLand generator. Through this model, users can acquire diverse corresponding depth maps from single segmentation input.

Local: Segment-wise depth shift. Here, we suggest a simple method to edit the selected global depth map. We observed that the semantic label ‘sky’ have smaller depth values than the semantic label ‘grass’. In other words, the local depth value can be shifted to a certain level only to the extent that the relative depth order of semantics does not change. Under this constraint, we show that shifting the depth of local parts can change the local view of a landscape. The representative example is depicted in Figure 1.

3.3. Two-phase inference

As a final inference model, we suggest a ‘2-phase inference’ as shown in Figure 3. It consists of two StyLand generators, i.e., S2D and SD2I. The depth maps are synthesized from user drawn semantic segmentation map by the first generator (Phase1), and both segmentation and selected depth are passed to the second generator to produce final landscape image (Phase2). Note that one can now easily get the desired depth map by selecting a candidate from diverse depth suggestions and by editing it locally. Since depth map mainly determines the structure of a landscape, the proposed inference model can be divided into ‘structure selection’ and ‘style selection’, respectively.

4. Experiments and Results

Implementation details. Our StyLandGAN uses an input image size of 256×256 for all experiments. The shape of the random latent code is set to $w \in \mathbb{R}^{64 \times 8 \times 8}$. We use the ADAM optimizer with $(\beta_1, \beta_2) = (0.0, 0.99)$, with a learning rate of 0.002, and a batch size of 8.

Dataset. Like all other previous methods [3, 18, 22, 23], we also scrape landscape images from flickr.com to construct a dataset named Flickr-Landscape. We randomly collected 48K images as a training set and 1K images as a test set. To build a segmentation-depth pair sets, we use the monocular depth estimation module [20], and semantic segmentation estimation module [32].

Baselines. To compare the performance of the proposed method, we first select previous segmentation-to-image(S2I) translation models: Pix2PixHD [31], SPADE [22], CC-FPSE [17], and OASIS [28]. Secondly, we extended Pix2Pix and SPADE for the SD2I translation task to compare our model fairly. The same concatenation approach for multi-modal inputs is applied to all methods.

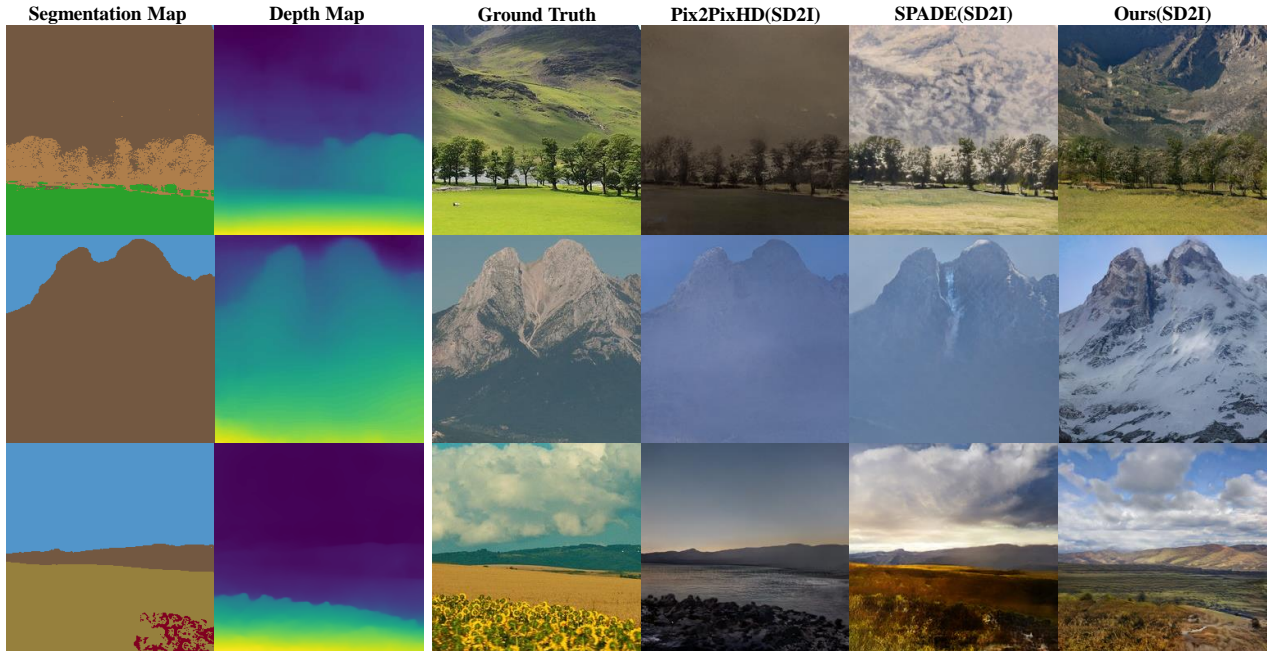


Figure 4. Qualitative comparison of SD2I translation model on Flickr-Landscape. Our model produces images with higher visual quality. More results are shown in supplementary materials.

S2I Model	FID(↓)	LPIPS(↑)	RMSE(-)
Pix2PixHD [31]	56.08	N/A	9.40
SPADE [22]	47.34	0.39	9.43
CC-FPSE [17]	48.43	0.18	9.29
OASIS [28]	31.92	<u>0.51</u>	9.34
StyLandGAN (Ours)	<u>34.50</u>	0.56	9.36

SD2I Model	FID(↓)	LPIPS(↑)	RMSE(↓)
Pix2PixHD [31]	48.22	N/A	<u>8.95</u>
SPADE [22]	<u>43.33</u>	<u>0.23</u>	9.10
StyLandGAN (Ours)	33.60	0.45	8.80

Table 1. Quantitative results of S2I and SD2I (Phase2 of 2-phase inference) model on Flickr-Landscape. The best scores are highlighted in bold, and the second-best are underlined. The arrow ↓ (or ↑) indicates that a lower (or higher) score is better.

Metrics. As other I2I models, we adopt FID [8] to measure ‘image quality’. We evaluate the ‘image diversity’ by calculating the mean LPIPS [34] distance between generated images. For each test image, we calculated the mean distance between 10 randomly generated images with fixed semantic and depth maps. We also measure ‘depth accuracy’ by using RMSE [30] between the depth map of the original image and the depth map of the synthesized image.

Results. In Table 1, we present the summarized compar-

ison results on S2I and SD2I translation separately. Note that Pix2PixHD can generate only a single image, and depth accuracy results on the S2I models are attached for reference. For the S2I model, StyLandGAN shows comparable score to other models. For the SD2I model, the proposed method achieves the best score in terms of FID, LPIPS, and RMSE. More importantly, we can observe the effectiveness of depth map as an additional information by comparing results between S2I and SD2I model. The depth guidance restricts the amount of randomness (image diversity) and enforces to generate intended representation (depth accuracy). Thus, for the SD2I model, the overall image diversity and depth accuracy score decreased compared to the S2I model. As shown in Figure 4, our model produces landscape images corresponding to input semantic map, and synthesizes more details in the virtue of plausible linear and planar representations from depth map.

5. Conclusion

In this paper, we present a novel conditional landscape synthesis framework, StyLandGAN, with depth map which is capable of expressing ridge and scale representation. We show that our ‘2-phase inference’ makes it possible to acquire diverse structure and style of landscape images in a row. Our framework exceeds previous I2I translation method in image quality, image diversity, and depth-accuracy.

References

- [1] Wengling Chen and James Hays. Sketchygan: Towards diverse and realistic sketch to image synthesis. In *The IEEE Conference on Computer Vision and Pattern Recognition (CVPR)*, June 2018. 2
- [2] Yunjey Choi, Youngjung Uh, Jaejun Yoo, and Jung-Woo Ha. Stargan v2: Diverse image synthesis for multiple domains. In *Proceedings of the IEEE Conference on Computer Vision and Pattern Recognition*, 2020. 2
- [3] Patrick Esser, Robin Rombach, and Björn Ommer. Taming transformers for high-resolution image synthesis, 2020. 2, 3
- [4] Rahul Garg, Neal Wadhwa, Sameer Ansari, and Jonathan T. Barron. Learning single camera depth estimation using dual-pixels. *ICCV*, 2019. 1
- [5] Clément Godard, Oisín Mac Aodha, Michael Firman, and Gabriel J. Brostow. Digging into self-supervised monocular depth prediction. October 2019. 1
- [6] Ian Goodfellow, Jean Pouget-Abadie, Mehdi Mirza, Bing Xu, David Warde-Farley, Sherjil Ozair, Aaron Courville, and Yoshua Bengio. Generative adversarial nets. In Z. Ghahramani, M. Welling, C. Cortes, N. Lawrence, and K. Q. Weinberger, editors, *Advances in Neural Information Processing Systems*, volume 27. Curran Associates, Inc., 2014. 1, 3
- [7] Aaron Hertzmann. Why do line drawings work? A realism hypothesis. *CoRR*, abs/2002.06260, 2020. 1
- [8] Martin Heusel, Hubert Ramsauer, Thomas Unterthiner, Bernhard Nessler, and Sepp Hochreiter. Gans trained by a two time-scale update rule converge to a local nash equilibrium. In *Advances in Neural Information Processing Systems 30: Annual Conference on Neural Information Processing Systems 2017*, 2017. 4
- [9] Xun Huang, Ming-Yu Liu, Serge Belongie, and Jan Kautz. Multimodal unsupervised image-to-image translation. In *ECCV*, 2018. 2
- [10] Xun Huang, Arun Mallya, Ting-Chun Wang, and Ming-Yu Liu. Multimodal conditional image synthesis with product-of-experts gans. In *Proc. CVPR*, 2021. 2
- [11] Phillip Isola, Jun-Yan Zhu, Tinghui Zhou, and Alexei A Efros. Image-to-image translation with conditional adversarial networks. *CVPR*, 2017. 2
- [12] Tero Karras, Samuli Laine, Miika Aittala, Janne Hellsten, Jaakko Lehtinen, and Timo Aila. Analyzing and improving the image quality of StyleGAN. In *Proc. CVPR*, 2020. 3
- [13] Hyunsu Kim, Yunjey Choi, Junho Kim, Sungjoo Yoo, and Youngjung Uh. Exploiting spatial dimensions of latent in gan for real-time image editing. In *Proceedings of the IEEE Conference on Computer Vision and Pattern Recognition*, 2021. 2, 3
- [14] Junho Kim, Minjae Kim, Hyeonwoo Kang, and Kwang Hee Lee. U-gat-it: Unsupervised generative attentional networks with adaptive layer-instance normalization for image-to-image translation. In *International Conference on Learning Representations*, 2020. 2
- [15] Hsin-Ying Lee, Hung-Yu Tseng, Jia-Bin Huang, Maneesh Kumar Singh, and Ming-Hsuan Yang. Diverse image-to-image translation via disentangled representations. In *European Conference on Computer Vision*, 2018. 2
- [16] Hsin-Ying Lee, Hung-Yu Tseng, Qi Mao, Jia-Bin Huang, Yu-Ding Lu, Maneesh Kumar Singh, and Ming-Hsuan Yang. Dri++: Diverse image-to-image translation via disentangled representations. *International Journal of Computer Vision*, pages 1–16, 2020. 2
- [17] Xihui Liu, Guojun Yin, Jing Shao, Xiaogang Wang, and Hongsheng Li. Learning to predict layout-to-image conditional convolutions for semantic image synthesis. In *Advances in Neural Information Processing Systems*, 2019. 2, 3, 4
- [18] Elizaveta Logacheva, Roman Suvorov, Oleg Khomenko, Anton Mashikhin, and Victor Lempitsky. Deeplandscape: Adversarial modeling of landscape videos. In *Proceedings of the European Conference on Computer Vision (ECCV)*, August 2020. 3
- [19] Lars Mescheder, Sebastian Nowozin, and Andreas Geiger. Which training methods for gans do actually converge? In *International Conference on Machine Learning (ICML)*, 2018. 3
- [20] S. Mahdi H. Miangoleh, Sebastian Dille, Long Mai, Sylvain Paris, and Yağız Aksoy. Boosting monocular depth estimation models to high-resolution via content-adaptive multi-resolution merging. 2021. 1, 3
- [21] Cooper Nederhood, Nicholas Kolkin, Deqing Fu, and Jason Salavon. Harnessing the conditioning sensorium for improved image translation. In *Proceedings of the IEEE/CVF International Conference on Computer Vision (ICCV)*, pages 6752–6761, October 2021. 2
- [22] Taesung Park, Ming-Yu Liu, Ting-Chun Wang, and Jun-Yan Zhu. Semantic image synthesis with spatially-adaptive normalization. In *Proceedings of the IEEE Conference on Computer Vision and Pattern Recognition*, 2019. 1, 2, 3, 4
- [23] Taesung Park, Jun-Yan Zhu, Oliver Wang, Jingwan Lu, Eli Shechtman, Alexei A. Efros, and Richard Zhang. Swapping autoencoder for deep image manipulation. In *Advances in Neural Information Processing Systems*, 2020. 2, 3
- [24] Aditya Ramesh, Mikhail Pavlov, Gabriel Goh, Scott Gray, Chelsea Voss, Alec Radford, Mark Chen, and Ilya Sutskever. Zero-shot text-to-image generation. In Marina Meila and Tong Zhang, editors, *Proceedings of the 38th International Conference on Machine Learning*, volume 139 of *Proceedings of Machine Learning Research*, pages 8821–8831. PMLR, 18–24 Jul 2021. 2
- [25] René Ranftl, Katrin Lasinger, David Hafner, Konrad Schindler, and Vladlen Koltun. Towards robust monocular depth estimation: Mixing datasets for zero-shot cross-dataset transfer. *IEEE Transactions on Pattern Analysis and Machine Intelligence (TPAMI)*, 2020. 1
- [26] Scott Reed, Zeynep Akata, Xinchun Yan, Lajanugen Logeswaran, Bernt Schiele, and Honglak Lee. Generative adversarial text to image synthesis. In Maria Florina Balcan and Kilian Q. Weinberger, editors, *Proceedings of The 33rd International Conference on Machine Learning*, volume 48 of *Proceedings of Machine Learning Research*, pages 1060–1069, New York, New York, USA, 20–22 Jun 2016. PMLR. 2
- [27] Kuniaki Saito, Kate Saenko, and Ming-Yu Liu. Coco-funit: Few-shot unsupervised image translation with a content con-

- ditioned style encoder. *arXiv preprint arXiv:2007.07431*, 2020. 2
- [28] Edgar Schönfeld, Vadim Sushko, Dan Zhang, Juergen Gall, Bernt Schiele, and Anna Khoreva. You only need adversarial supervision for semantic image synthesis. In *International Conference on Learning Representations*, 2021. 2, 3, 4
- [29] Ming Tao, Hao Tang, Songsong Wu, Nicu Sebe, Fei Wu, Xiao-Yuan Jing, and Bingkun Bao. Df-gan: Deep fusion generative adversarial networks for text-to-image synthesis. *arXiv preprint arXiv:2008.05865*, 2020. 2
- [30] Igor Vasiljevic, Nick Kolkin, Shanyi Zhang, Ruotian Luo, Haochen Wang, Falcon Z. Dai, Andrea F. Daniele, Mohammadreza Mostajabi, Steven Basart, Matthew R. Walter, and Gregory Shakhnarovich. DIODE: A Dense Indoor and Outdoor DEpth Dataset. *CoRR*, abs/1908.00463, 2019. 4
- [31] Ting-Chun Wang, Ming-Yu Liu, Jun-Yan Zhu, Andrew Tao, Jan Kautz, and Bryan Catanzaro. High-resolution image synthesis and semantic manipulation with conditional gans. In *Proceedings of the IEEE Conference on Computer Vision and Pattern Recognition*, 2018. 2, 3, 4
- [32] Hang Zhang, Chongruo Wu, Zhongyue Zhang, Yi Zhu, Zhi Zhang, Haibin Lin, Yue Sun, Tong He, Jonas Muller, R. Manmatha, Mu Li, and Alexander Smola. Resnest: Split-attention networks. *arXiv preprint*, 2020. 3
- [33] Pan Zhang, Bo Zhang, Dong Chen, Lu Yuan, and Fang Wen. Cross-domain correspondence learning for exemplar-based image translation. In *Proceedings of the IEEE/CVF Conference on Computer Vision and Pattern Recognition*, pages 5143–5153, 2020. 2
- [34] Richard Zhang, Phillip Isola, Alexei A Efros, Eli Shechtman, and Oliver Wang. The unreasonable effectiveness of deep features as a perceptual metric. In *CVPR*, 2018. 3, 4
- [35] Jiapeng Zhu, Yujun Shen, Deli Zhao, and Bolei Zhou. In-domain gan inversion for real image editing. In *Proceedings of European Conference on Computer Vision (ECCV)*, 2020. 3
- [36] Jun-Yan Zhu, Richard Zhang, Deepak Pathak, Trevor Darrell, Alexei A Efros, Oliver Wang, and Eli Shechtman. Toward multimodal image-to-image translation. In *Advances in Neural Information Processing Systems*, 2017. 2
- [37] Peihao Zhu, Rameen Abdal, Yipeng Qin, and Peter Wonka. Sean: Image synthesis with semantic region-adaptive normalization. In *IEEE/CVF Conference on Computer Vision and Pattern Recognition (CVPR)*, June 2020. 2

Supplementary materials for StyLandGAN: A StyleGAN based Landscape Image Synthesis using Depth-map

A. Additional comparison with previous works

PoE-GAN. Recently, a conditional image synthesis framework called PoE-GAN has been proposed. Through PoE-GAN, it adopts various input modalities, and even handles contradictory modalities. StyLandGAN currently uses a fixed number of modalities, and it is hard to properly reflect the results of applying contradictory conditions. Though PoE-GAN can probably be extended to incorporate depth maps, StyLandGAN has the advantage of creating contents in a progressive way. Our ‘2-phase inference’ first translates a segmentation map, which is two-dimensional information, into a depth map, which is three-dimensional information. In each phase, our model suggests various styles while fixing previous constraints. By separating structure and style selection process within two different phases, StyLandGAN has the great advantage of allowing users to progressively embody their ideas and intentions into the landscape image to be synthesized.

Taming Transformers. We find that the Taming Transformers (T.T) tries a depth map input condition for image synthesis tasks. Even though T.T only tried synthesizing images with the main subject like birds and dogs, we assume this model could be extended to synthesize landscape images. However, our StyLandGAN not only focuses on using a depth map to synthesize landscape images but also suggests synthesizing various depth maps with ‘two-phase inference’. Moreover, we find that our Stylegan-based architecture makes inference much faster than T.T.

B. S2D translation result analysis

Our S2D translation model should produce a plausible depth map to properly generate a final image. To verify the effectiveness of S2D translation model, we illustrate the depth distribution of the synthesized images and ground truth (GT) images. We extracted depth from Flickr-landscape test set as a ground-truth, and translated depth from semantic segmentation of test set. We divide the depth distribution of each segmentation label to observe each tendency. The distribution of the average depth value for each semantic label is shown in Fig 2. The x -axis represents the mean depth value of an image, where 0 represents the near area and 255 represents the far area. The y -axis represents the number of images. More overlaps between two distributions means that the estimated depth are similar to the ground truth, hence, realistic. Furthermore, we can also see the intuition that the sky is furthest, the mountains are closer than the sky, and the other semantics such as tree, grass, and earth lie almost everywhere in an landscape image.

C. Additional qualitative examples

We show extensive qualitative results in this section. Fig 3 illustrates the advantage of a depth map by comparing S2I and SD2I translation models. Fig 4 shows the additional qualitative results of SD2I translation models with other baselines. More results on our ‘2-phase Inference’ framework are shown in Fig 5. Lastly, we show advantage in Fig 6.

D. Limitation

Although our model obtains convincing results in terms of both qualitative and quantitative evaluations compared to other models, we find out that StyLandGAN model does not work well when expressing close objects as depicted in Fig 1. Our model fails to produce plausible image due to the unrealistic depth map synthesized from segmentation of cluttered objects such as trees.

In addition, it is difficult to perfectly control the perspective of objects only by shifting the value of depth. For a more dramatic and more realistic editing of an object, its size also should be changed according to its depth value at the same time. We leave this point as future work for the development of content creation tools utilizing a depth map.

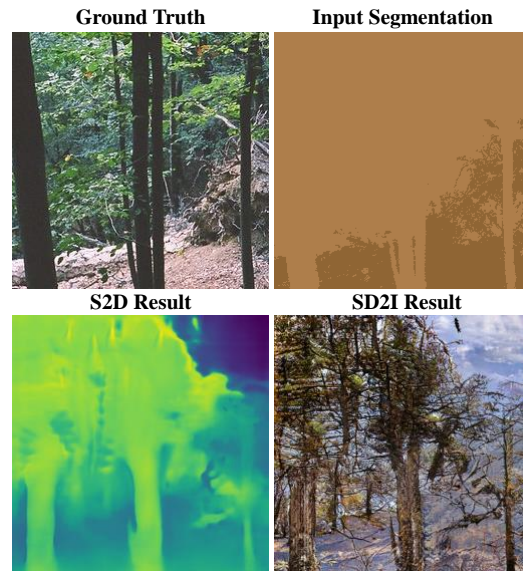


Figure 1. Example of our model when conditioned on close objects. Our S2D and SD2I translation models both have limitations when the object is too close to the camera.

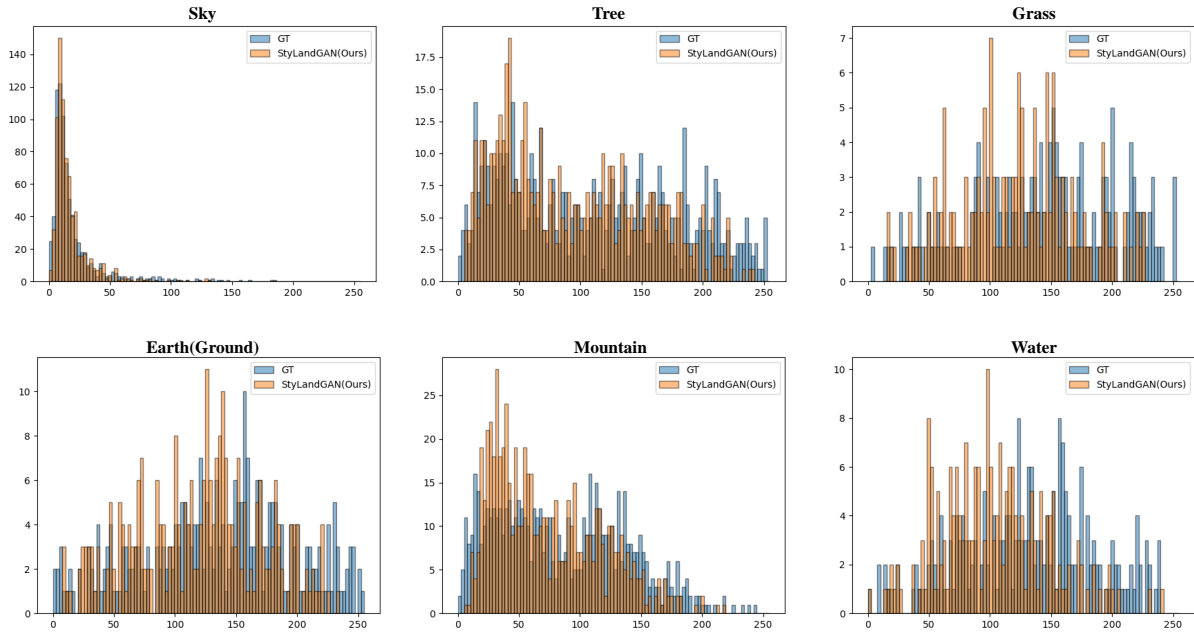


Figure 2. Distribution of mean depth maps for each representative segmentation label. We compare the depth value of the ground truth (GT) and the S2D translation result. Note that the S2D translation model synthesizes an almost similar depth distribution as GT.

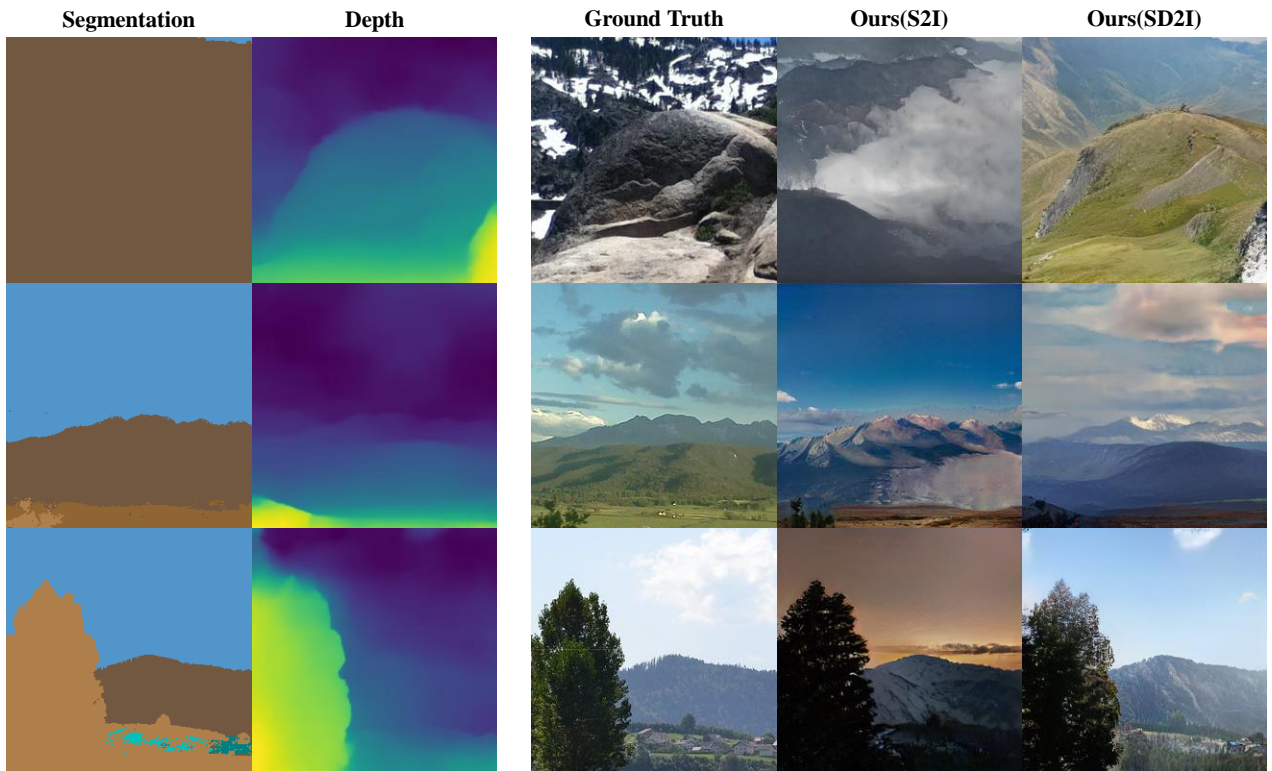


Figure 3. Example of generated StyLandGAN results trained on S2I and SD2I translation models. Note that even if a specific structure cannot be expressed in the segmentation map as in the first row, the depth map can have a more detailed expressions.

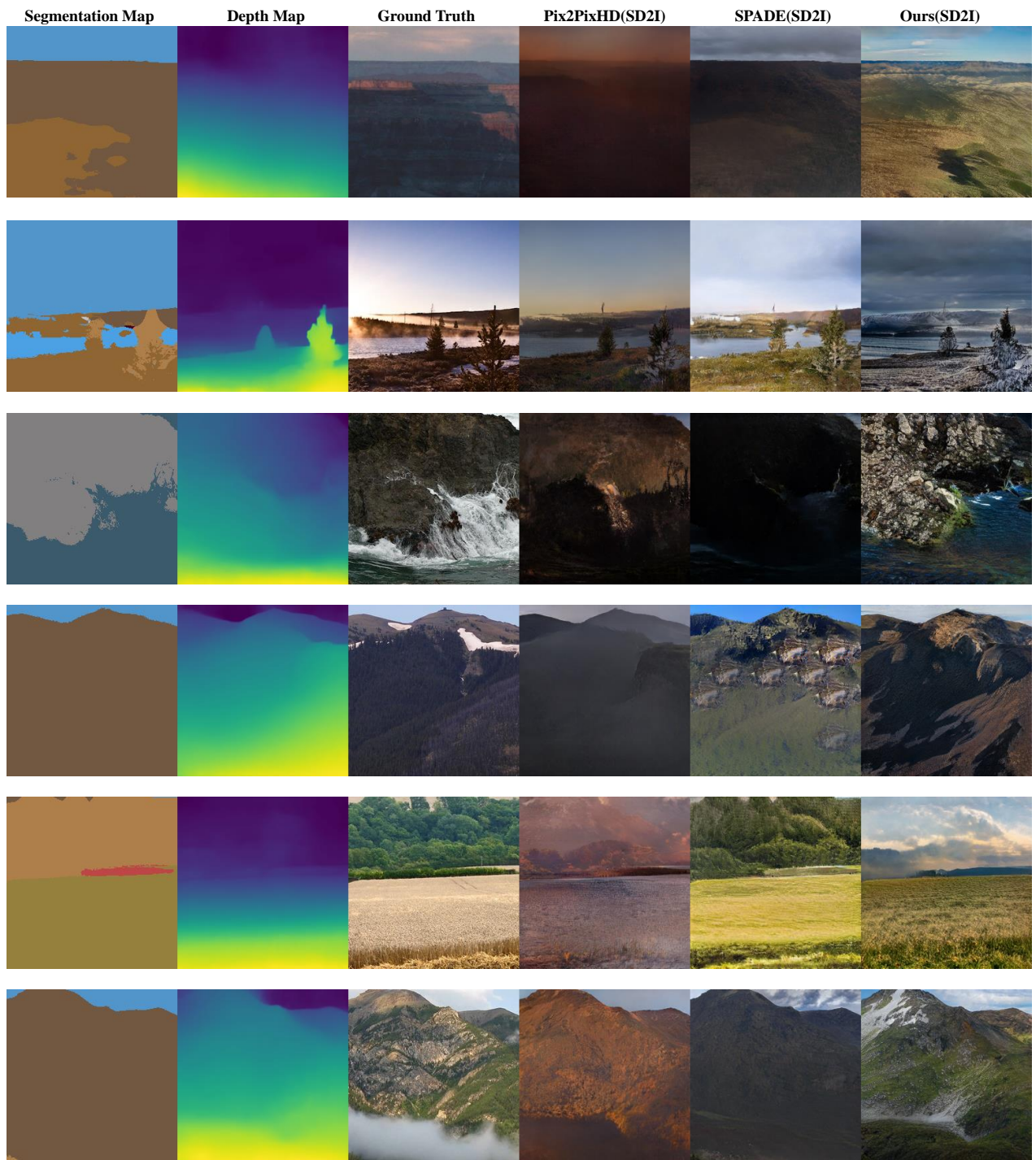


Figure 4. Additional qualitative comparisons of SD2I translation model on Flickr-landscape.

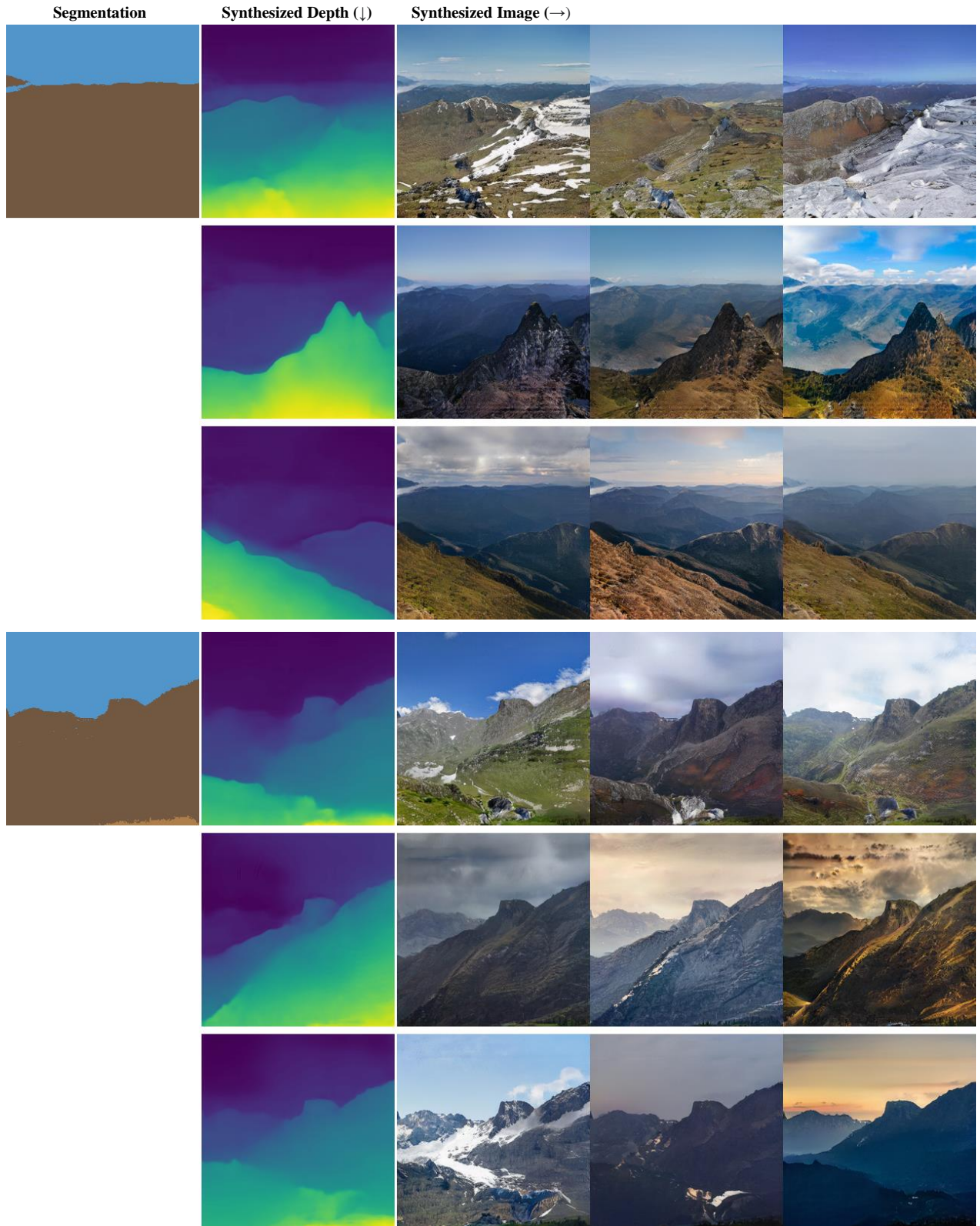


Figure 5. Additional results of ‘2-phase inference’. The S2D translation model takes the first column images and generates various depth maps as in the second column. With the first and second images, the SD2I translation model generates multimodal stylized outputs.

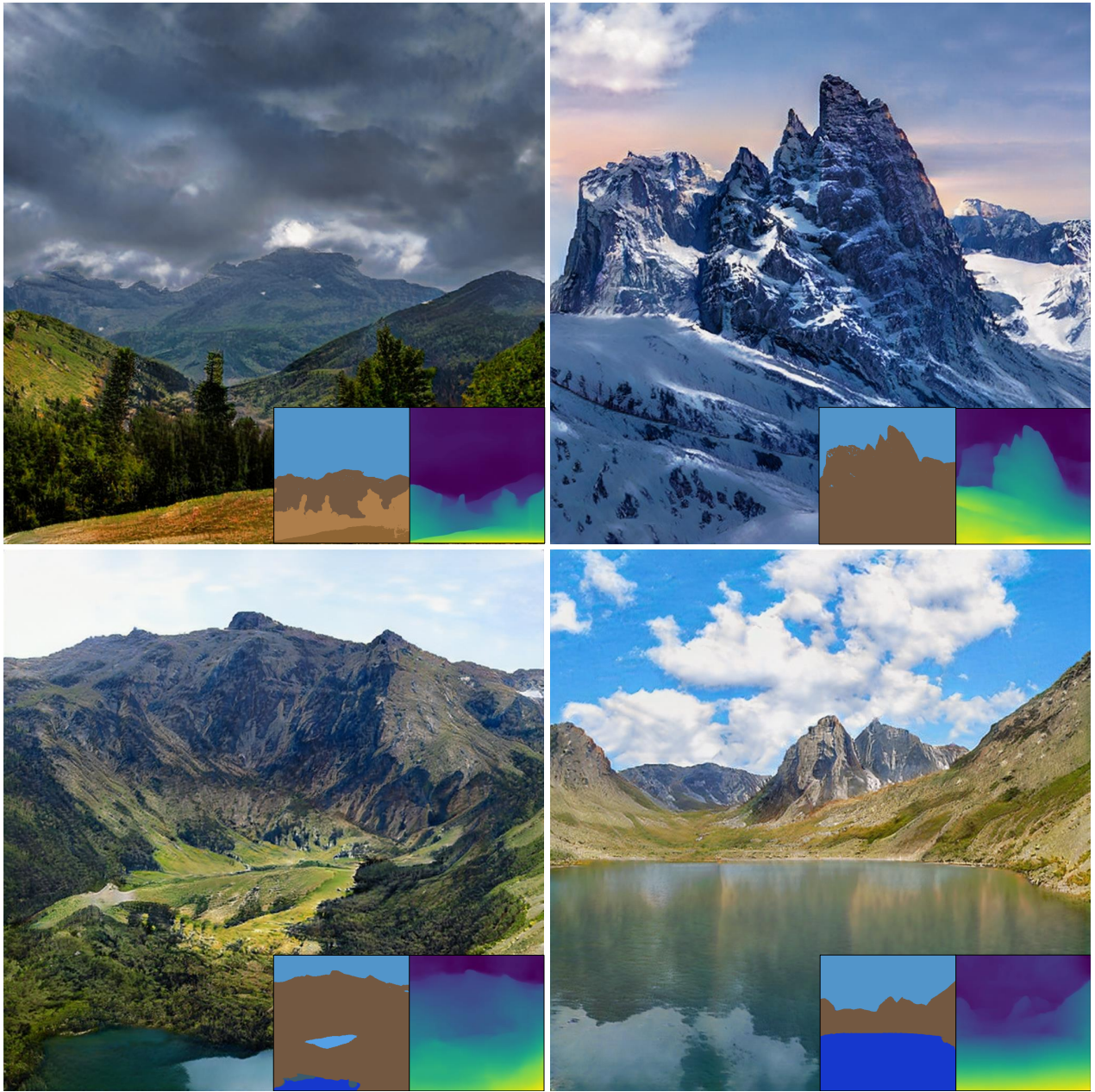


Figure 6. Examples of high resolution (1024×1024) image synthesis with the SD2I translation model. Conditions are shown on the bottom right of the corner, which is extracted from the real landscape image.